



OPEN ACCESS

EDITED BY

Sathishkumar Kuppusamy,
Bharathidasan University, India

REVIEWED BY

Ananthaselvam Azhagesan,
VIT University, India
Praveen Kumar,
University of Ljubljana, Slovenia

*CORRESPONDENCE

Deepak Sahu,
✉ sahud@nitj.ac.in

RECEIVED 24 June 2024

ACCEPTED 08 August 2024

PUBLISHED 22 August 2024

CITATION

Verma S, Sahu D and Almutairi BO (2024)
Production and characterization of biodiesel
fuel produced from third-generation
feedstock.
Front. Mater. 11:1454120.
doi: 10.3389/fmats.2024.1454120

COPYRIGHT

© 2024 Verma, Sahu and Almutairi. This is an open-access article distributed under the terms of the [Creative Commons Attribution License \(CC BY\)](https://creativecommons.org/licenses/by/4.0/). The use, distribution or reproduction in other forums is permitted, provided the original author(s) and the copyright owner(s) are credited and that the original publication in this journal is cited, in accordance with accepted academic practice. No use, distribution or reproduction is permitted which does not comply with these terms.

Production and characterization of biodiesel fuel produced from third-generation feedstock

Suraj Verma¹, Deepak Sahu^{1*} and Bader O. Almutairi²

¹Department of Chemical Engineering, Dr B. R. Ambedkar National Institute of Technology, Jalandhar, Punjab, India, ²Department of Zoology, College of Science, King Saud University, Riyadh, Saudi Arabia

Biodiesel is an eco-friendly, renewable alternative fuel, and it can be obtained from soybean oil, vegetable oils, animal fat, or microalgae. This study presents a comprehensive investigation into the production and characterization of microalgae biodiesel utilizing multiple analytical techniques, including CHNSO analysis, Fourier-transform infrared spectroscopy (FTIR), gas chromatography–mass spectrometry (GC–MS), and proton nuclear magnetic resonance spectroscopy (¹H NMR). The CHNSO analysis revealed the elemental composition of biodiesel blends, highlighting the effects of TiO₂ nanoparticle concentrations on carbon, nitrogen, sulfur, and oxygen content. With increasing TiO₂ concentration, a steady increase in the carbon content and a gradual decrease in the nitrogen content were observed. According to the CHNSO analysis, the sulfur content of blended biodiesel was found to be lower than that of fossil diesel, with an empirical formula of CH_{2.26}N_{0.000584}S_{0.000993}O_{0.0517}. FTIR and ¹H NMR spectroscopy confirmed the synthesis of biodiesel. Fourier-transform infrared resonance confirmed the presence of ester groups at 1732 cm⁻¹, and a prominent peak at 1,455 cm⁻¹ indicated a higher carbon content in the blended biodiesel. GC–MS analysis identified compounds of fatty acid methyl esters (FAMES) and hydrocarbons. The major components of FAMES were 9-octadecenoic acid methyl ester (C₁₉H₃₆O₂), linoleic acid ethyl ester (C₂₀H₃₆O₂), and hexadecanoic acid methyl ester (C₁₇H₃₄O₂), with compositions 20.65%, 9.67%, and 6.26%, respectively. The presence of methyl ester in the blended fuel suggests its potential as an alternative fuel source.

KEYWORDS

biodiesel, titanium dioxide, characterization, CHNSO, Fourier-transform infrared spectroscopy, gas chromatography–mass spectrometry, proton nuclear magnetic resonance, fatty acid methyl esters

1 Introduction

The continuous economic and population growth significantly change the lifestyle and lead to a significant increase in energy consumption. The primary source of energy is dependent on fossil fuels such as petroleum products and coal. However, the rapid depletion of these non-renewable resources and their associated environmental impacts, including the exhaustion of harmful gases, has necessitated the development of more sustainable and eco-friendly energy sources. Biodiesel can be used as a sustainable renewable fuel resource that can substitute fossil fuels. It offers several advantages, including low emissions, biodegradability, non-toxicity, good lubricity, and

sustainability. Notably, biodiesel's potential to provide energy security is particularly significant for agriculture-based countries like India. Biofuels come in different types, including edible oil biofuels and non-edible oil biofuels. Although edible oil biofuels are produced from food crops and can alter food supplies, non-edible oil biofuels, such as algae-based biofuels, offer a more sustainable alternative. Algae, as a third-generation biofuel, do not require farmable land and are abundant in carbohydrates, polypeptide, lipids, and oil content. Their potential for biodiesel production is significant due to their ability to grow in various aqueous environments and high yield for biofuel production. Microalgae, which can grow in various water bodies, including sewage water, pure water, salty water, or highly polluted water, have emerged as a potential source for biofuel production. Their ability to utilize sunlight, CO₂, and water to produce lipids, along with their short harvesting life cycle and high yield for biofuel production, makes them a promising option. Additionally, microalgae have the capability to remove nutrients and pollutants from water, further enhancing their environmental benefits.

Transitioning to renewable energy sources, such as biodiesel produced from algae, offers a promising solution to the environmental challenges posed by conventional fossil fuels. Bio-based diesel is a sustainable and renewable fuel for internal combustion engine prepared from various sources like soybean oil, vegetable oils, or animal fat which meet the predefined ASTM D-6751 standard (Nautiyal et al., 2014), and its properties were determined by the physicochemical properties and calorific value of the fuel according to ISO norms (Demirbas, 2009). Black soldier fly larvae are used as a potential substitute fuel for diesel engines and can be used in blends with diesel like B25, B50, B75, and B100. Their brake thermal efficiency improved by 8.21%, whereas the trend of NO_x emissions decreased compared to diesel fuel (Kamarulzaman et al., 2019). *Camelus dromedarius*, a low cost Hachi fat, can be a promising source for biofuel production (Sbihi et al., 2014). Oil from fish waste is converted into biodiesel by enzymatic catalysis and optimized by surface methodology (Ching-Velasquez et al., 2020). Inam et al. found the novel feedstock *Koelreuteria paniculata*, which was a non-edible source with a high oil yield from their biomass that was 28%–30% with a low free fatty acid content of 0.91% (Khan et al., 2020). Mandarin (Citrus reticulata) seeds can be transformed into biodiesel, which was asserted via ¹H NMR spectroscopy, hydrogen nuclear magnetic resonance, and ultimate analysis. Its empirical formula is given by CH_{1.88}, O_{0.16}, N_{0.012}, and S_{0.0005} with the heating value of 37.96 MJ/kg (Fadhil, 2021). Kumar et al. worked on two different algae, namely, *monoraphidium sp* and *Chlorella sorokiniana*, for energy generation. They found that *in situ* growing of *C. sorokiniana* has a better yield than the other, and found a higher lipid profile, reduced CO and HC emissions, and greater brake thermal efficiency (Namitha et al., 2021). Ahmend et al. used alumina nanoparticles (Al₂O₃) to make jojoba biodiesel blends with diesel blends in the ratio of 20% jojoba biodiesel to 80% diesel, with varying concentrations of Al₂O₃ nanoadditive. Utilization of Al₂O₃ nanoparticles improves engine performance, decreases the brake-specific fuel consumption, and reduces exhaust emissions. In jojoba oil, biodiesel blending of 20 mg/L Al₂O₃ improves engine performance (El-Seesy et al., 2018). Coconut oil extraction is done by the cold extrusion process from coconuts bought. The FTIR

result shows that various functional components were present in the biodiesel prepared from coconut oil. Fatty acid methyl ester (67.8%) was confirmed via gas chromatography and mass spectroscopy in coconut oil biodiesel (Ekeoma et al., 2023). Bibin et al. (2020) worked on punnai oil for its conversion into biodiesel via the transesterification process. Punnai oil biodiesel has better combustion properties due to the presence of linoleic, oleic, and palmitic fatty acid, which were confirmed via gas chromatography. Lal ambari is a novel feedstock for biodiesel production, which had a high brake thermal efficiency of 4.4% higher than diesel but increased CO₂ emissions by 3.5% (Shrivastava and Verma, 2020). Saravanan et al. (2020) used mahua and rapeseed biodiesel in equal proportion and found that 20% of the dual biodiesel from mahua and rapeseed gave the best results. Rajak et al. (2020) used a Spirulina microalgae biodiesel blend with diesel. A 20% microalgae biodiesel blend with diesel produces lower exhaust emissions than fossil diesel. However, the increase in fuel consumption was 3.2%, and BTE was hampered by 3.03% at maximum load. Ahmed et al. used leather industry waste fat for biodiesel production, and this methyl ester was mixed with diesel in 10%–30%. They have a similar cetane number, but their injection time was longer than that of other biodiesel (Keskin et al., 2020). Non-consumable vegetable oils like Roselle and Karanja oil can act as prominent alternatives for biodiesel production and can be blended with diesel. Their brake thermal efficiency was lowered by 1.5% and 2.8%, respectively, compared with diesel; for Roselle, biodiesel was lowered by 10%, and for Karanja, biodiesel was lowered by 10% (Shrivastava et al., 2020). Isobutanol biodiesel blended with diesel had better evaporation and atomization, so it improved the combustion characteristics of blended fuels, but NO_x emissions were significantly influenced by the mixing of isobutanol at medium and maximum loads (Xiao et al., 2020). Qamar et al. (2023) used the TiO₂ nanoparticles, which were efficient for biodiesel production of up to 98%. Shelare et al. (2023) stated that the use of nanoadditive in biodiesel could potentially improve the properties of biodiesel fuel. Hoang et al. (2023) expressed that the micro-algal biomass deposited a higher extent of oil than other land-based plant species. Blending biodiesel from 0% to 20% in the diesel reduced the exhaust gas emissions, that is, CO, SOX, and HC (Tizvir et al., 2023).

A few works have been performed on the production and characterization of biofuel from third-generation feedstock. Microalgae-based biodiesel offers a sustainable alternative to fossil fuel due to its high oil yield and ability to grow on non-arable land and in wastewater. It reduces dependency on fossil fuels, has a lower carbon footprint, can utilize waste CO₂, and contributes to sustainable development, which are the main advantages of microalgae biofuels. Therefore, the present research work is focused on the production and characterization of biofuel produced from third-generation feedstock. This investigation utilized various techniques, including FTIR analysis, CHNSO analysis, GC–MS analysis, and H NMR analysis.

2 Material and methods

2.1 Preparation of biodiesel

Wet microalgae (third generation) biomass was collected and placed in direct sunlight for 8–10 days to remove moisture content.

Once dried, the biomass was ground into a powdered form, and oil was extracted from it. Biodiesel was then synthesized from the microalgae oil through the transesterification process, using methanol and sodium hydroxide (NaOH) as catalysts. Subsequently, blending was carried out in a ratio of 50:25:25, comprising diesel (D), microalgae biodiesel (MB), and butanol (BT), respectively. To optimize the properties of the blended fuel, a TiO₂ additive was introduced in different amounts in the blended sample. The prepared fuel sample includes the following: MB25BT25, MB25BT25 TiO₂ (20ppm), MB25BT25 TiO₂ (50ppm), MB25BT25 TiO₂ (80ppm), and MB25BT25 TiO₂ (110ppm). The production method is mentioned in the paper (Verma et al., 2023).

2.2 Characterization

2.2.1 CHNS analysis

The Thermo FLASH-2000 elemental CHNSO analyzer was utilized to analyze the typical organic elements, including carbon, hydrogen, nitrogen, sulfur, and oxygen. A sample of 1.0 mg was placed in a tin boat array and subjected to heating at 980 °C while being exposed to a continuous and consistent flow of helium-enriched oxygen gas to proportionally assess the compositional elements of C, H, N, S, and O. The percentage composition was determined through the application of the difference method.

2.2.2 Fourier transform-infrared spectroscopy

The Agilent Technologies Fourier transform spectrometer, FTIR 4100 ExoScan model, was employed to obtain mid-infrared spectra of the biodiesel blend. The micro-lab software facilitated the process, whereas the FTIR spectrometer utilized a diamond-attenuated total reflectance (ATR) sample interface system, eliminating the need for a sample cell. Samples were introduced onto the diamond interface smoothly. Each spectrum was promptly captured within seconds at the aim of 4 cm⁻¹, span of 4,000 cm⁻¹–500 cm⁻¹, with a minimal sample volume requirement of no more than 0.5 mL per sample. Ethanol was used for cleaning purposes, particularly to cleanse the sample crystal prior to testing the sample. The scan outputs were then obtained as spectra on the integrated computer system.

2.2.3 Gas chromatography and mass spectroscopy analysis

Fatty acid methyl esters (FAMES) were investigated via GC–MS spectroscopy, employing a GCMS-QP2020 provided with a quadrupole mass spectrometer utilizing electron impact ionization. Separation of FAMES was achieved using an Rxi-5sil MS capillary column (30 m long and 0.25 mm diameter, with a thickness of 0.25), with injector and column temperatures at 265°C and 250°C, respectively. The recognition of various FAMES was accomplished by comparing their profiles with those stored in the NIST Library, serving as a reference for interpreting the peaks in the GC spectrum.

2.2.4 Proton nuclear magnetic resonance

¹H NMR spectroscopy was used to determine the chemical structure of potential compounds, emphasizing hydrogen atom

analysis. The ¹H NMR spectra were acquired using a JEOL (ECS-400) 400 MHz NMR spectrometer equipped with both broadband (BB) and inverse (BBI) probes.

For sample preparation, approximately 5–10 mg of biodiesel were dissolved in 0.7–0.8 mL of CDCl₃ (trichloro (deutero) methane), with the internal reference tetramethylsilane (TMS). Variables such as relaxation delay (D1) and receiver gain (RG) were meticulously adjusted to optimize performance. At the same time, the 90° pulse width was gauged to ensure adequate relaxation of the nuclei for quantitative spectra acquisition, as outlined in prior studies (Kumar et al., 2014; Sarpal et al., 2015). The 90° pulse width (PW) was individually calibrated for each sample, with a relaxation delay (D1) of 10 s, a 90° pulse width (P1) ranging from 8.13 to 8.64 microseconds, and multiple scans (NS) set at either 16 or 32. The chemical shift range was configured from 0 to 9 ppm. All spectra underwent three-time integration following appropriate phase and baseline corrections, with the average integral areas utilized for quantitative analysis.

3 Results and discussion

The blended biodiesel was characterized with the help of CHNSO analysis, FTIR analysis, GC–MS analysis, and ¹H NMR analysis.

3.1 CHNSO analysis

The CHNSO analysis of a biodiesel blend determines the mass concentration of carbon, hydrogen, nitrogen, sulfur, and oxygen. As the concentration of TiO₂ nanoparticles increases in the biodiesel, the percentage of carbon steadily rises. This phenomenon may enhance combustion efficiency, promoting complete combustion of carbon-based fuels like biodiesel. Conversely, the nitrogen content decreases gradually with increasing TiO₂ nanoparticle concentrations in the biodiesel. This decrease is attributed to the catalytic effect of TiO₂, which potentially facilitates the conversion of nitrogen oxides (NO_x) into less harmful nitrogen species during combustion. The CHNSO composition of biodiesel blend and fossil diesel is given in Table 1.

MB25BT25, as shown in Table 1, was abbreviated by a prepared test biodiesel blend, which had a fixed percentage of butanol of 25%, biodiesel of 25%, and 50% diesel in it but had varying concentrations of TiO₂. Table 1 shows that blended biodiesel has lower oxygen (5.469%) than MB25BT25, indicating that MB25BT25 TiO₂ (110 ppm) has a higher CV value than MB25BT25 and less than conventional diesel fuel. It is observed that the present MB25BT25 TiO₂ (100 ppm) biodiesel blend has low sulfur content, which generates significantly less emission of (SO_x) after burning in diesel engines. The CHNSO analysis also indicates that the empirical formula of the biodiesel is approximately CH_{2.26}N_{0.000584}S_{0.000993}O_{0.0517}. Based on these findings, it was revealed that the current blended biodiesel is more advantageous for diesel engine applications. Butanol has a higher energy content (around 29.2 MJ/L) than ethanol (21.2 MJ/L), making it a more energy-rich fuel, which means that butanol can provide more energy

TABLE 1 CHNSO composition (mass) of different blends of microalgae biodiesel with TiO₂.

Element	MB25BT25	MB25BT25 TiO ₂ (20ppm)	MB25BT25 TiO ₂ (50ppm)	MB25BT25 TiO ₂ (80ppm)	MB25BT25 TiO ₂ (110ppm)	Fossil diesel
Carbon (C)	72.163	74.521	76.102	78.23	79.215	85.98
Hydrogen (H)	9.121	11.216	12.630	13.782	14.892	13.72
Nitrogen (N)	0.181	0.112	0.091	0.073	0.054	0.00
Sulfur (S)	0.009	0.015	0.051	0.102	0.210	0.30
Oxygen (O)	18.416	13.966	11.016	7.673	5.469	0.00

TABLE 2 Functional group frequencies of recognized biodiesels.

Wavenumber (cm ⁻¹)	Types of vibration	Functional group	References
3,340	Stretching	O-H (alcohols), amines, and phenols	Chen et al. (2016)
3,082–2,860	Asymmetrical stretching	C-H (alkanes)	Carrillo et al. (2004), Kumar et al. (2014)
2,345	Stretching	C = C alkynes	Carrillo et al. (2004)
1732	Stretching	C = O (ester carbonyl functional group in FAME)	Mahamuni and Adewuyi (2009)
1,455–1,345	Bending and rocking	C-H (methyl or -CH ₃)	Coates (2000)
1,300–1,000	Stretching	= C-H, -CH ₂ -OH, C-O alkoxy esters, ethers, and C-OC	Siatis et al. (2006), Wahab et al. (2010), Coates (2000)
950	Out of plane bending	= C-H (trans-disubstituted alkene)	Coates (2000)
738	Bending of alkenes and overlapping of rocking vibration of methylene	= C-H and -(CH ₂) _n methylene groups (cis-disubstituted alkenes and aromatic)	Mahamuni and Adewuyi (2009), Carrillo et al. (2004), Coates (2000)

per liter, leading to better fuel efficiency and longer driving ranges. It is also less hygroscopic and can be transported through existing pipelines.

3.2 FTIR spectroscopy

Fourier-transform infrared spectroscopy (FTIR) is a powerful analytical technique for identifying organic, polymeric, and inorganic substances. It analyzes test samples to understand their chemical characteristics. The generated spectrum is used to identify functional groups in the fuel sample, providing qualitative insights into its composition and associated vibrational modes. The functional groups present in biodiesel are listed in Table 2.

Figure 1 represents the FTIR pattern of microalgae biodiesel blends within the wave number span of 500 cm⁻¹–4,000 cm⁻¹. The magnitude of peaks at various wavenumbers indicates the presence of functional groups. At 3,340 cm⁻¹, there is a weak

peak in the biodiesel, confirming the occurrence of amines and O-H stretching vibrations, which signify the occurrence of alcohols and phenols (Chen et al., 2016). The peaks between 3,082 cm⁻¹ and 2,860 cm⁻¹ are attributed to C-H vibrations, indicating the occurrence of alkanes in the biodiesel (Islam et al., 1999; Carrillo et al., 2004).

Biodiesel exhibits a weak peak at 2,345 cm⁻¹, attributed to alkynes stretching. The peak at 1732 cm⁻¹ shows the C = O stretch, confirming the existence of ester groups in the biodiesel (Mahamuni and Adewuyi, 2009). The prominent peak at 1,455 cm⁻¹ in blended biodiesel indicates a higher carbon content in biodiesel. Furthermore, peaks lower than 1,000 cm⁻¹, owing to C = C stretching, result from aromatic and C-X stretching. Peaks within the bandwidth of 1,000 cm⁻¹ and 1,300 cm⁻¹ are recognized to O-CH₂-C and -CH₂-OH stretching (Siatis et al., 2006; Wahab et al., 2010). Overall, the FTIR analysis of biodiesel validates the presence of diverse components such as alkenes, alkanes, aromatics, ketones, phenolic, aldehydes, and carboxylic acids.

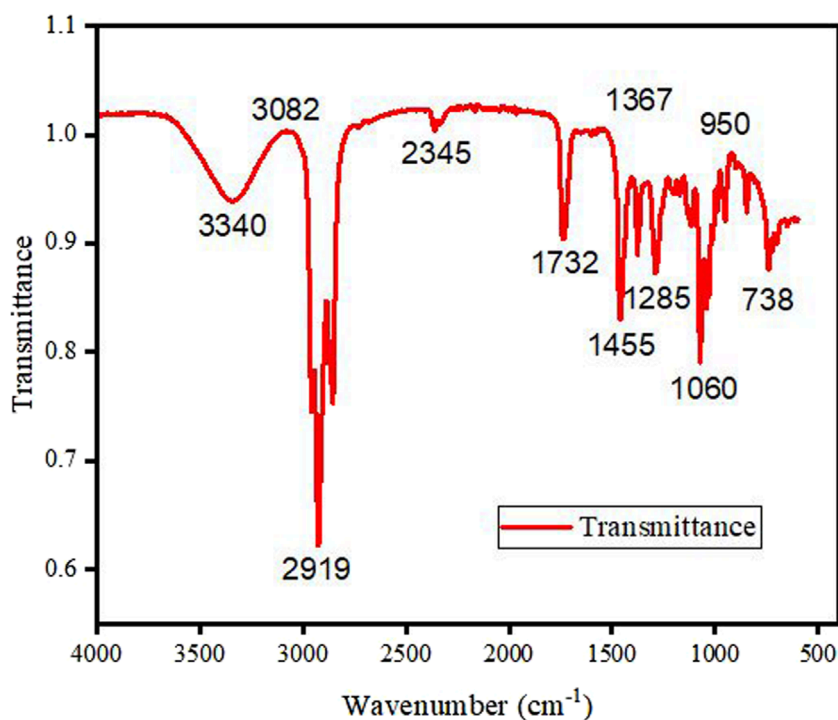


FIGURE 1 FTIR spectra of biodiesel.

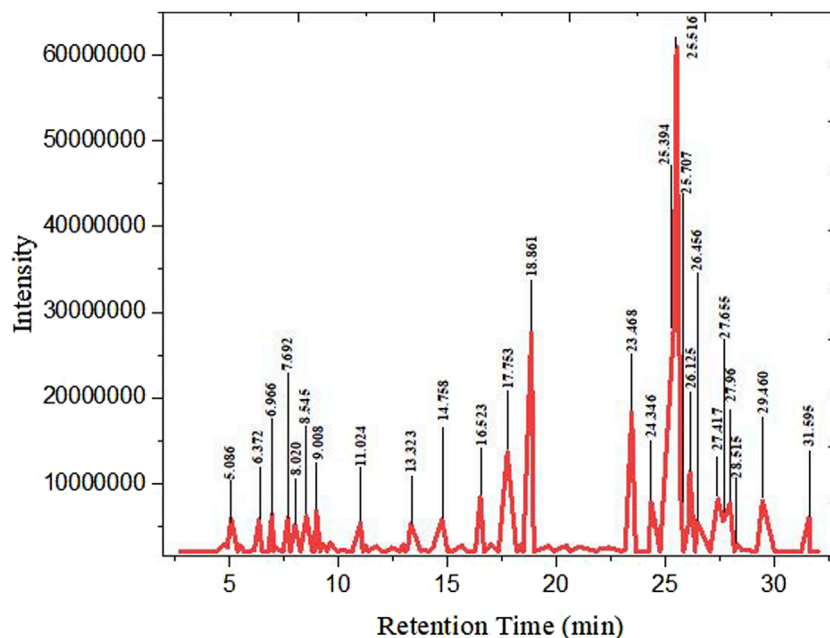


FIGURE 2 Reconstructed plot of GC-MS results of biodiesel.

3.3 GC-MS analysis

The compounds found in the blended biodiesel were identified through the GC-MS analysis using the NIST Library (National

Institute of Standards and Technology). The data suggest the presence of multiple components, with several peaks detected in the biodiesel spectra, indicating the possible existence of additional compounds in trace amounts.

TABLE 3 Major compounds in microalgae biodiesel.

Peak No.	Retention time (min)	Peak area (%)	Chemical formula	Molar mass	Chemical compound
1	5.086	2.05	C ₁₂ H ₁₈	162	Benzene, (3,3-dimethylbutyl-)
2	6.372	1.97	C ₁₉ H ₃₆ O ₄	328	Oxalic acid, 2-ethylhexyl nonyl ester
3	6.966	2.22	C ₁₈ H ₃₀	246	Benzene, (1,3,3-trimethylnonyl)
4	7.692	2.06	C ₉ H ₁₂	120	Mesitylene
5	8.02	1.76	C ₂₀ H ₃₀ O ₂	302	Hydratropic acid, undec-2-en-1-yl ester
6	8.545	2.12	C ₁₈ H ₃₆	252	Dodecane, 2-cyclohexyl-
7	9.008	2.31	C ₁₅ H ₂₂ O ₂	234	Hydratropic acid, isohexyl ester
8	11.024	1.84	C ₂₀ H ₃₂ O ₂	304	Butyric acid, 2-Phenyl-, dec-2-yl ester
9	13.323	1.84	C ₁₄ H ₃₀	198	Dodecane, 4,6-dimethyl-
10	14.758	1.99	C ₁₅ H ₃₂	212	Dodecane, 2,6,10-trimethyl-
11	16.523	2.89	C ₁₀ H ₁₀ O ₄	194	Dimethyl phthalate
12	17.753	4.68	C ₁₁ H ₁₂ O ₄	208	1,2-benzenedicarboxylic acid, ethyl methyl ester
13	18.861	9.45	C ₁₂ H ₁₄ O ₄	222	Diethyl phthalate
14	23.468	6.26	C ₁₇ H ₃₄ O ₂	270	Hexadecanoic acid, methyl ester
15	24.346	2.69	C ₂₀ H ₄₂	282	Eicosane
16	25.394	9.67	C ₂₀ H ₃₆ O ₂	308	Linoleic acid ethyl ester
17	25.516	20.85	C ₁₉ H ₃₆ O ₂	296	9-octadecenoic acid, methyl ester
18	25.707	2.94	C ₁₉ H ₃₈ O ₂	298	Methyl stearate
19	26.05	1.70	C ₂₀ H ₃₆ O ₂	308	Linoleic acid ethyl ester
20	26.125	3.87	C ₂₀ H ₃₈ O ₂	310	Ethyl oleate
21	26.456	1.92	C ₂₁ H ₄₄	296	Heneicosane
22	27.417	2.580	C ₂₇ H ₅₆	380	2-methylhexacosane
23	27.655	1.92	C ₂₁ H ₄₂ O ₂	326	Eicosanoic acid, methyl ester
24	27.96	2.63	C ₂₂ H ₄₂ O ₂	338	Oleic acid, butyl ester
25	28.515	0.78	C ₂₇ H ₅₄ O ₂	410	Hexacosanoic acid, methyl ester
26	29.46	2.73	C ₂₃ H ₄₆ O ₂	354	Docosanoic acid, methyl ester
27	31.595	2.10	C ₂₅ H ₅₀ O ₂	382	Tetracosanoic acid, methyl ester

Figure 2 illustrates the key components for streamlining the GC–MS analysis data for clarity and conciseness. The analysis identified 27 major compounds, as elaborated in Table 3. Comparing peak retention times and peak area percentages between the

chromatograms of the biodiesel samples and the standard facilitates peak identification and quantification.

Various hydrocarbon compounds were observed in the GC–MS analysis, along with remaining peaks and compounds containing

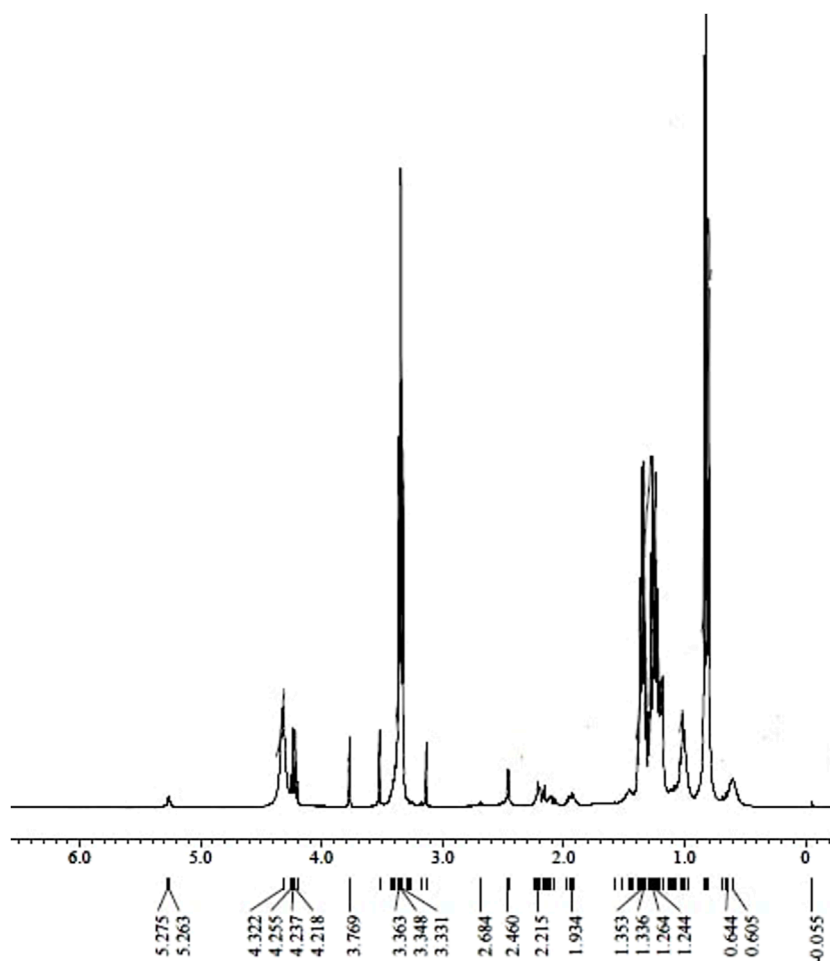


FIGURE 3
 ^1H NMR spectra of biodiesel.

oxygen atoms. Most of these were classified as fatty acid methyl esters, associated with biodiesel standards. The peak at number 27, with a peak area of 2.10%, is significant due to tetracosanoic acid methyl ester ($\text{C}_{25}\text{H}_{50}\text{O}_2$) having a molecular weight of 382 g/mol. The analysis predominantly showed the presence of methyl palmitate, methyl stearate, diethyl phthalate, methyl oleate, and methyl linoleate in biodiesel, resulting from the conversion of esters from microalgae oil to biodiesel, as reported by Naik et al. (2011).

Microalgae biodiesel has a higher potential for use as an alternative fuel because it contains a significant amount of methyl oleate (9-octadecenoic acid methyl ester) in more substantial quantities than other algae biofuels. The presence of long-chain fatty acid methyl oleate in biodiesel is significant as it appears to improve the cold flow properties of the fuel. The methyl ester compositions in biodiesel blends produced from the blending of microalgae biodiesel, butanol, and diesel with nanoadditive titanium dioxide indicate the presence of 9-octadecenoic acid methyl ester ($\text{C}_{19}\text{H}_{36}\text{O}_2$), linoleic acid ethyl ester ($\text{C}_{20}\text{H}_{36}\text{O}_2$), and hexadecanoic acid methyl ester ($\text{C}_{17}\text{H}_{34}\text{O}_2$) at compositions of 20.65%, 9.67%, and 6.26%, respectively.

Other esters found in the biodiesel include 1,2-benzenedicarboxylic acid, ethyl methyl ester ($\text{C}_{11}\text{H}_{12}\text{O}_4$), oleic

acid butyl ester ($\text{C}_{22}\text{H}_{42}\text{O}_2$), and hexacosanoic acid methyl ester ($\text{C}_{27}\text{H}_{54}\text{O}_2$), with percentages of 4.68%, 2.63%, and 0.78%, respectively. It is evident from the analysis that the presence of C17, C19, and C20 (methyl ester compounds) is higher, indicating that microalgae-based biodiesel has the potential to serve as an alternative to fossil fuels.

The presence of higher concentrations of oleic and palmitic acids in the blended biodiesel fuel showed better oxidative stability and cetane value of the fuel, which imparted low NOx emissions. Oleic acid content in biofuels indicates ignition quality, combustion heat, viscosity, and lubricity (Gouda Narayan et al., 2018). Methyl ester fuels with higher cetane numbers typically consist of high amounts of saturated fatty acids such as palmitic, stearic, and behenic acid (docosanoic acid, methyl ester) (Knothe et al., 1998), which have the highest cetane numbers.

3.4 ^1H NMR spectroscopy

FTIR spectroscopy was used to observe the functional group of microalgae biodiesel. However, FTIR spectroscopy is limited in quantifying the presence of specific components at particular

wavenumbers. Therefore, to enhance the understanding of specific components, ^1H NMR analysis was conducted. The hydrogen nuclear magnetic resonance (HNMR) of biodiesel analyzes the presence of different types of protons by their chemical shift, as depicted in Figure 3.

The H NMR analysis revealed distinct peaks corresponding to various proton environments in biodiesel. Methoxy protons exhibited a singlet peak at 3.63 ppm, whereas $\alpha\text{-CH}_2$ proton singlet was detected at 2.46 ppm, affirming the occurrence of methyl esters. Additionally, peaks at 0.83 ppm indicated the existence of methyl protons, whereas a prominent peak between 1.23 ppm and 1.36 ppm represented methylene protons within the carbon chain. The occurrence of α -carbonyl methylene protons was evidenced by peaks at 2.215 ppm. A sharp peak at 3.65 ppm further confirmed the presence of methyl esters (Monteiro et al., 2009). Peaks at 5.2 ppm were attributed to olefinic hydrogen. Notably, the absence of peaks between 6.0 and 9.0 ppm suggested minimal aromatics in the biodiesel, which is indicative of higher quality (Mokhlisse et al., 1999).

4 Conclusion

The proposed work focused on the comprehensive investigation of the characteristics of blended biodiesel produced from microalgae oil. Various characterization techniques are employed:

1. CHNSO analysis reveals the elemental composition, showing variations with the addition of TiO_2 nanoparticles. The resulting biodiesel exhibits lower sulfur content than diesel, suggesting improved combustion efficiency and reduced emissions. The CHNSO result shows that the empirical formula for the present fuel is $\text{CH}_{2.26}\text{N}_{0.000584}\text{S}_{0.000993}\text{O}_{0.0517}$.
2. FTIR analysis confirms the occurrence of functional groups in biodiesel, including alcohols, alkanes, alkynes, esters, and other compounds. The formation of ester groups is validated through absorption peaks at 1732 cm^{-1} and a prominent peak at $1,455\text{ cm}^{-1}$, indicating a higher carbon content in the biodiesel sample.
3. GC-MS analysis elucidates the chemical composition, highlighting the presence of fatty acid methyl esters and methyl oleate, which suggests favorable fuel properties.
4. ^1H NMR analysis provides detailed information about proton environments, confirming the presence of methyl esters and other compounds.

TiO_2 provides a large surface area for the transesterification reaction, which improves the conversion of triglycerides (oils) into methyl esters (biodiesel). TiO_2 -catalyzed biodiesel has lower emissions of harmful pollutants like carbon monoxide and particulates, making it a more environmentally friendly alternative to traditional diesel fuel. The comprehensive characterization underscores the potential of microalgae biodiesel as a sustainable

alternative fuel to fossil fuels, offering valuable insights into its composition and properties.

Data availability statement

The original contributions presented in the study are included in the article/Supplementary Material; further inquiries can be directed to the corresponding author.

Author contributions

SV: conceptualization, formal analysis, investigation, methodology, and writing—original draft. DS: conceptualization, formal analysis, investigation, supervision, writing—original draft, and writing—review and editing. BA: funding acquisition, project administration, resources, validation, visualization, and writing—review and editing.

Funding

The authors declare that financial support was received for the research, authorship, and/or publication of this article. The work was supported by Researchers Supporting Project, number RSP2024R414, King Saud University, Riyadh, Saudi Arabia.

Acknowledgments

The authors acknowledge the support of King Saud University, Riyadh, Saudi Arabia, Researchers Supporting Project number (RSP2024R414).

Conflict of interest

The authors declare that the research was conducted in the absence of any commercial or financial relationships that could be construed as a potential conflict of interest.

Publisher's note

All claims expressed in this article are solely those of the authors and do not necessarily represent those of their affiliated organizations, or those of the publisher, the editors, and the reviewers. Any product that may be evaluated in this article, or claim that may be made by its manufacturer, is not guaranteed or endorsed by the publisher.

References

- Bibin, C., Seeni, K. P., and Devan, P. K. (2020). Performance, emission and combustion characteristics of a direct injection diesel engine using blends of punnai oil biodiesel and diesel as fuel. *Therm. Sci.* 24 (1A), 13–25. doi:10.2298/tsci180325233b
- Carrillo, E., Colom, X., Sunol, J. J., and Saurina, J. (2004). Structural FTIR analysis and thermal characterisation of lyocell and viscose-type fibres. *Eur. Polym. J.* 40 (9), 2229–2234. doi:10.1016/j.eurpolymj.2004.05.003

- Chen, W., Shi, S., Zhang, J., Chen, M., and Zhou, X. (2016). Co-pyrolysis of waste newspaper with high-density polyethylene: synergistic effect and oil characterization. *Energy Convers. Manag.* 112, 41–48. doi:10.1016/j.enconman.2016.01.005
- Ching-Velasquez, J., Fernández-Lafuente, R., Rodrigues, R. C., Plata, V., Rosales-Quintero, A., Torrestiana-Sánchez, B., et al. (2020). Production and characterization of biodiesel from oil of fish waste by enzymatic catalysis. *Renew. Energy* 153, 1346–1354. doi:10.1016/j.renene.2020.02.100
- Coates, J. (2000). Interpretation of infrared spectra, a practical approach. *Encycl. Anal. Chem.* 12, 10815–10837.
- Demirbas, A. (2009). Characterization of biodiesel fuels. *Energy Sources, Part A* 31 (11), 889–896. doi:10.1080/15567030801904202
- Ekeoma, M. O., Wirnkor, V. A., Emmanuel, I. C., Ngozi, V. E., and Ezichi, M. N. I. (2023). Production and characterization of biodiesel from coconut (cocos nucifera) oil. *Chem. Res. J.* 8, 45–53.
- El-Seesy, A. I., Attia, A. M., and El-Batsh, H. M. (2018). The effect of Aluminum oxide nanoparticles addition with Jojoba methyl ester-diesel fuel blend on a diesel engine performance, combustion and emission characteristics. *Fuel* 224, 147–166. doi:10.1016/j.fuel.2018.03.076
- Fadhil, A. B. (2021). Production and characterization of liquid biofuels from locally available nonedible feedstocks. *Asia-Pacific J. Chem. Eng.* 16 (1), e2572. doi:10.1002/apj.2572
- Gouda Narayan, P. A. K., Singh, R. K., and Ratha, S. K. (2018). Pyrolytic conversion of protein rich microalgae *Arthrospira platensis* to bio-oil. *Res. J. Chem. Environ.* 22, 12.
- Hoang, A. T., Sirohi, R., Pandey, A., Nizetić, S., Lam, S. S., Chen, W. H., et al. (2023). Biofuel production from microalgae: challenges and chances. *Phytochem. Rev.* 22 (4), 1089–1126. doi:10.1007/s11101-022-09819-y
- Islam, M. N., Zailani, R., and Ani, F. N. (1999). Pyrolytic oil from fluidised bed pyrolysis of oil palm shell and its characterisation. *Renew. Energy* 17 (1), 73–84. doi:10.1016/s0960-1481(98)00112-8
- Kamarulzaman, M. K., Hafiz, M., Abdullah, A., Chen, A. F., and Awad, O. I. (2019). Combustion, performances and emissions characteristics of black soldier fly larvae oil and diesel blends in compression ignition engine. *Renew. Energy* 142, 569–580. doi:10.1016/j.renene.2019.04.126
- Keskin, A., Şen, M., and Emiroğlu, A. O. (2020). Experimental studies on biodiesel production from leather industry waste fat and its effect on diesel engine characteristics. *Fuel* 276, 118000. doi:10.1016/j.fuel.2020.118000
- Khan, I. U., Yan, Z., and Chen, J. (2020). Production and characterization of biodiesel derived from a novel source *Koelerutera paniculata* seed oil. *Energies* 13 (4), 791. doi:10.3390/en13040791
- Knothe, G., Bagby, M. O., and Ryan III, T. W. (1998). Precombustion of fatty acids and esters of biodiesel. A possible explanation for differing cetane numbers. *J. Am. Oil Chemists' Soc.* 75 (8), 1007–1013. doi:10.1007/s11746-998-0279-1
- Kumar, R., Bansal, V., Patel, M. B., and Sarpal, A. S. (2014). Compositional analysis of algal biomass in a nuclear magnetic resonance (NMR) tube. *J. Algal Biomass Util.* 5, 36–45.
- Mahamuni, N. N., and Adewuyi, Y. G. (2009). Fourier transform infrared spectroscopy (FTIR) method to monitor soy biodiesel and soybean oil in transesterification reactions, petrodiesel–biodiesel blends, and blend adulteration with soy oil. *Energy and Fuels* 23 (7), 3773–3782. doi:10.1021/ef900130m
- Mokhlisse, A., Chanãa, M. B., and Chanãa, M. (1999). Effect of water vapor on the pyrolysis of the Moroccan (Tarfaya) oil shale. *J. Anal. Appl. Pyrolysis* 48 (2), 65–76. doi:10.1016/s0165-2370(98)00108-9
- Monteiro, M. R., Ambrozini, A. R. P., Liao, L. M., and Ferreira, A. G. (2009). Determination of biodiesel blend levels in different diesel samples by ¹H NMR. *Fuel* 88 (4), 691–696. doi:10.1016/j.fuel.2008.10.010
- Naik, C. V., Westbrook, C. K., Herbinet, O., Pitz, W. J., and Mehl, M. (2011). Detailed chemical kinetic reaction mechanism for biodiesel components methyl stearate and methyl oleate. *Proc. Combust. Inst.* 33 (1), 383–389. doi:10.1016/j.proci.2010.05.007
- Namitha, B., Sathish, A., Kumar, P. S., Nithya, K., and Sundar, S. (2021). Micro algal biodiesel synthesized from *Monoraphidium* sp., and *Chlorella sorokiniana*: feasibility and emission parameter studies. *Fuel* 301, 121063. doi:10.1016/j.fuel.2021.121063
- Nautiyal, P., Subramanian, K. A., and Dastidar, M. G. (2014). Production and characterization of biodiesel from algae. *Fuel Process. Technol.* 120, 79–88. doi:10.1016/j.fuproc.2013.12.003
- Qamar, O. A., Jamil, F., Hussain, M., Bae, S., Inayat, A., Shah, N. S., et al. (2023). Advances in synthesis of TiO₂ nanoparticles and their application to biodiesel production: a review. *Chem. Eng. J.* 460, 141734. doi:10.1016/j.cej.2023.141734
- Rajak, U., Nashine, P., and Verma, T. N. (2020). Effect of spirulina microalgae biodiesel enriched with diesel fuel on performance and emission characteristics of CI engine. *Fuel* 268, 117305. doi:10.1016/j.fuel.2020.117305
- Saravanan, A., Murugan, M., Reddy, M. S., and Parida, S. (2020). Performance and emission characteristics of variable compression ratio CI engine fueled with dual biodiesel blends of Rapeseed and Mahua. *Fuel* 263, 116751. doi:10.1016/j.fuel.2019.116751
- Sarpal, A. S., Silva, S. R., Silva, P. R., Monteiro, T. V., Itacolomy, J., Cunha, V. S., et al. (2015). Direct method for the determination of the iodine value of biodiesel by quantitative nuclear magnetic resonance (q¹H NMR) spectroscopy. *Energy and Fuels* 29 (12), 7956–7968. doi:10.1021/acs.energyfuels.5b01462
- Sbihi, H. M., Nehdi, I. A., Tan, C. P., and Al-Resayes, S. I. (2014). Production and characterization of biodiesel from *Camelus dromedarius* (Hachi) fat. *Energy Convers. Manag.* 78, 50–57. doi:10.1016/j.enconman.2013.10.036
- Shelare, S. D., Belkhole, P. N., Nikam, K. C., Jathar, L. D., Shahapurkar, K., Soudagar, M. E. M., et al. (2023). Biofuels for a sustainable future: examining the role of nano-additives, economics, policy, internet of things, artificial intelligence and machine learning technology in biodiesel production. *Energy* 128874. doi:10.1016/j.energy.2023.128874
- Shrivastava, P., and Verma, T. N. (2020). An experimental investigation into engine characteristics fueled with Lal ambari biodiesel and its blends. *Therm. Sci. Eng. Prog.* 17, 100356. doi:10.1016/j.tsep.2019.100356
- Shrivastava, P., Verma, T. N., Samuel, O. D., and Pugazhendhi, A. (2020). An experimental investigation on engine characteristics, cost and energy analysis of CI engine fuelled with Roselle, Karanja biodiesel and its blends. *Fuel* 275, 117891. doi:10.1016/j.fuel.2020.117891
- Siatis, N. G., Kimbaris, A. C., Pappas, C. S., Tarantilis, P. A., and Polissiou, M. G. (2006). Improvement of biodiesel production based on the application of ultrasound: monitoring of the procedure by FTIR spectroscopy. *J. Am. Oil Chemists' Soc.* 83 (1), 53–57. doi:10.1007/s11746-006-1175-1
- Tizvir, A., Molaieimesh, G. R., Zahedi, A. R., and Labbafi, S. (2023). Optimization of biodiesel production from microalgae and investigation of exhaust emissions and engine performance for biodiesel blended. *Process Saf. Environ. Prot.* 175, 319–340. doi:10.1016/j.psep.2023.05.056
- Verma, S., Upadhyay, R., Shankar, R., and Pandey, S. P. (2023). Performance and emission characteristics of micro-algae biodiesel with butanol and TiO₂ nano-additive over diesel engine. *Sustain. Energy Technol. Assessments* 55, 102975. doi:10.1016/j.seta.2022.102975
- Wahab, M. A., Jellali, S., and Jedidi, N. (2010). Ammonium biosorption onto sawdust: FTIR analysis, kinetics and adsorption isotherms modeling. *Bioresour. Technol.* 101 (14), 5070–5075. doi:10.1016/j.biortech.2010.01.121
- Xiao, H., Guo, F., Wang, R., Yang, X., Li, S., and Ruan, J. (2020). Combustion performance and emission characteristics of diesel engine fueled with iso-butanol/biodiesel blends. *Fuel* 268, 117387. doi:10.1016/j.fuel.2020.117387